Food Chemistry 298 (2019) 124973

Contents lists available at ScienceDirect

Food Chemistry

journal homepage: www.elsevier.com/locate/foodchem

Quantitative proteomics analysis reveals proteins and pathways associated with anthocyanin accumulation in barley

Guoqiang Zhang[a,b,1], Wenhua Xue[a,1], Jie Dai[d], Qijun Xu[b,c], Yulin Wang[b,c], Hongjun Yuan[b,c], Kun Yang[a,e], Yiman Qi[a,e], Xingquan Zeng[b,c,*], Tashi Nyima[b,f,*]

[a] College of Biological and Chemical Engineering, Anhui Polytechnic University, Wuhu, Anhui 241000, China
[b] State Key Laboratory of Barley and Yak Germplasm Resources and Genetic Improvement, Lhasa, Tibet 850002, China
[c] Research Institute of Agriculture, Tibet Academy of Agricultural and Animal Husbandry Sciences, Lhasa, Tibet 850002, China
[d] Shanghai Bioprofile Technology CO., LTD, Shanghai 200241, China
[e] College of Food Science and Engineering, Northwest A & F University, Yangling 712100, China
[f] Tibet Academy of Agricultural and Animal Husbandry Sciences, Lhasa, Tibet 850000, China

ARTICLE INFO

Keywords:
Highland barley
Color
Anthocyanin
Quantitative proteomics

ABSTRACT

The aim of the present study was to explore the underlying mechanisms involved in anthocyanin biosynthesis in purple, blue, and white barley using quantitative proteomics analysis. We identified the differences in protein expression and related functions involved in anthocyanin biosynthesis in purple, blue, and white barley (named H, M, and L groups, respectively, based on their anthocyanin content) using TMT-liquid chromatography/mass spectroscopy-based proteomic methods. Totally, 297, 300, 254, and 1421 differentially expressed proteins (DEPs) were found in H vs. L, H vs. M, L vs. M, and H vs. L vs. M groups, respectively. Six clusters of proteins from the 1421 DEPs were mainly involved in carbon metabolism, amino acid and secondary metabolite biosynthesis, and metabolic pathways. Several proteins were validated using parallel reaction monitoring. The proteins involved in amino acid biosynthesis, carbon metabolism, metabolic pathways, and phenylpropanoid biosynthesis were responsible for the color differences in the three barley varieties.

1. Introduction

Barley (*Hordeum vulgare* L.) is among the most ancient cereal plants of the grass family Poaceae and currently ranks fourth among cereals in worldwide production, behind maize (*Zea mays*), wheat, and rice (Shen et al., 2016). Barley grains are rich in protein, lysine, minerals, and carbohydrates, and have a high content of dietary fiber, especially soluble β-glucan, which may exert numerous physiological effects and inhibit cholesterol synthesis (Ewaschuk et al., 2012; Sima, Vannucci, & Vetvicka, 2018; Thandapilly, Ndou, Wang, Nyachoti, & Ames, 2018). With caryopses that thresh free from the pales, naked or dehulled barley is preferred for the food industry and human food consumption because it allows the omission of a processing step (Chen et al., 2014; Naceur, Cheikh-M'hamed, da Silva, & Abdelly, 2017). The kernel colors of barley varieties show great diversity at maturity, such as white, yellow, blue, purple, and black pigmentation, which is usually the result of a different pigment in the pericarp and aleurone layer because of phenolic compounds and anthocyanin content (Glagoleva et al., 2017; Mullick, Faris, Brink, & Acheson, 1958).

Anthocyanins belong to the water-soluble flavonoids and are the most important pigments that are responsible for most of the color diversity in plants (Lao, Sigurdson, & Giusti, 2017; Stuper-Szablewska & Perkowski, 2017). The anthocyanins present in cereals have many health benefits including anti-inflammatory, anti-oxidant, hepatoprotective, retina protective, neuroprotective, hypolipidemic, anti-glycemic, bodyweight regulatory, anti-cancer, and anti-aging properties (Zhu, 2018). Strygina et al. showed that the MYC-encoding gene (*HvMyc2*) was involved in anthocyanin synthesis underlying variation

Abbreviations: ANOVA, analysis of variance; BP, biological process; CC, cellular component; TMT, tandem mass tags; GO, gene ontology; KEGG, Kyoto Encyclopedia of Genes and Genomes; LC-MS/MS, liquid chromatography (LC)-mass spectrometry; MF, molecular function; PPI, protein-protein interaction; TCA, trichloroacetic acid; UA, urea

* Corresponding authors at: State Key Laboratory of Barley and Yak Germplasm Resources and Genetic Improvement; Tibet Academy of Agricultural and Animal Husbandry Sciences, Lhasa, Tibet, 850000, China (T. Nyima and X. Zeng).

E-mail addresses: zhangguoqiang@ahpu.edu.cn (G. Zhang), Jie.dai@bioprofile.cn (J. Dai), Yangkun12@nwsuaf.edu.cn (K. Yang), qiyiman@nwsuaf.edu.cn (Y. Qi), xingquanz_2@126.com (X. Zeng), Nyima_Tashi@163.com (T. Nyima).

[1] Guoqiang Zhang and Wenhua Xue should be regard as co-first authors.

https://doi.org/10.1016/j.foodchem.2019.124973
Received 5 January 2019; Received in revised form 24 May 2019; Accepted 9 June 2019
Available online 12 June 2019

in barley aleurone color (Strygina, Borner, & Khlestkina, 2017). A recent study demonstrated the regulatory function of the adenine nucleotide translocator-2 gene in anthocyanin biosynthesis in the grain pericarp of barley (Shoeva, Mock, Kukoeva, Borner, & Khlestkina, 2016). Nevertheless, little is known regarding the changes in protein expression that are involved in anthocyanin biosynthesis in barley grains of different colors.

Proteomics studies provide global detection and quantitation of proteins, and also detect protein-protein interactions (PPIs) of a given cell at a given time under specific conditions (Avin, Levy, Porat, & Abramson, 2017). Advances in liquid chromatography (LC)-high-resolution tandem mass spectrometry (MS)-based proteomic strategies enable large-scale protein identification and robust protein biomarker discoveries (Naryzhny, 2018). The emerging technology of quantitative proteomics allows for the systematic study of static state or perturbation-induced changes in proteome-wide expression profiling (Pan & Aebersold, 2007). Proteomics analysis has been utilized in the grain development research of barley (Finnie, Melchior, Roepstorff, & Svensson, 2002).

In the present study, tandem mass tags (TMT)-LC-MS/MS (Thompson et al., 2003) was applied to determine the levels of protein expression and related functions involved in anthocyanin biosynthesis in purple, blue, and white barley. Moreover, to validate candidate proteins, targeted method-parallel reaction monitoring (PRM) (Rauniyar, 2015; Ronsein et al., 2015) was used. Our findings provide a valuable picture of the physiological and molecular mechanisms of anthocyanin biosynthesis activity and provide resources for the identification of proteins to improve the concentration of anthocyanin in barley.

2. Materials and methods

2.1. Plant material and sampling

Three varieties of Tibetan hulless barley—purple barley, blue barley, and white barley—were provided by the Tibet Agriculture and Animal Husbandry University (Linzhi, Tibet, China). The color of barleys, from purple and blue to white, is related to anthocyanin levels; thus, the purple, blue, and white barley were named H (highest), M (moderate), and L (lowest) groups, respectively, in the present study. All the three hulless barley varieties were planted during 2017 and grown under normal environmental conditions (field natural environment), and received the same field management practices. The seeds have been sterilized before cultivation in 70% of ethanol for disinfect. Upon maturity, the harvested seed grains were stored at room temperature after natural drying. Three biological replicates were prepared for each group.

2.2. Quantitative analysis of anthocyanins

Anthocyanin extraction was conducted based on the method described by Kim et al. (2007). Each 0.2 g of the powdered whole grain sample was soaked in a conical flask (wrapped in aluminum foil) containing 2 mL of 80% methanol and 0.1% HCl for 24 h at 4 °C. The mixture was centrifuged at 10,000 × *g* for 10 min, and the supernatant was filtered through a 0.45 μm membrane filter (nylon, Titan) and transferred to an amber glass vial for avoiding light. Total anthocyanin content in grain samples was determined using the spectrophotometric method as previously described (Abdel-Aal & Hucl, 1999; Abdel-Aal, Young, & Rabalski, 2006).

2.3. Protein extraction

An appropriate amount of seed grains from each of the three groups were ground into powder using small amounts of liquid nitrogen. Approximately 20 mg of powder was taken from each sample group (H, M, and L), which was then added into 200 μL lysis buffer (4% sodium dodecyl sulfate (SDS), 100 mM Tris, 100 mM dithiothreitol (DTT), pH 7.8), sonicated, and precipitated overnight with trichloroacetic acid (TCA)-acetone solution at −20 °C. After centrifugation (16,000 × *g*, 1 min, 4 °C), the samples were washed twice with cold acetone, and air dried. Subsequently, 150 μL of the lysis buffer was added to each sample tube, sonicated, and the supernatant was extracted after centrifugation at 16,000 × *g* for 15 min. Protein quantification was performed using the bicinchonic acid assay. Approximately 20 μg of protein was taken from each group for SDS-PAGE analysis to evaluate the quantitative accuracy and to quantitate protein extraction.

2.4. Protein digestion and peptide desalination

Protein digestion was conducted using the filter-aided sample preparation method (Wiśniewski, 2016). Briefly, 300 μg of sample from each group was taken for protein digestion. We added DTT into the protein sample resulting in a final concentration of 100 mM and DTT reduction was conducted at 56 °C for 1 h. Then, after adding 200 μL of urea (UA) buffer (8 M UA and 150 mM Tris-HCl, pH 8.0), the samples were loaded on a 10 kDa ultrafiltration centrifuge tube, followed by centrifugation at 12,000 × *g* for 15 min, and the filtrate was discarded (this step was repeated once). Subsequently, the samples were alkylationed with 100 μL of iodoacetamide (IAA) (50 mM IAA in UA), shaken at 600 rpm for 1 min, and centrifuged at 12,000 × *g* for 10 min after 30 min at room temperature in darkness. Next, another 100 μL of UA buffer was added, and the samples were centrifuged at 12,000 × *g* for 10 min; we repeated this procedure twice. Subsequently, 100 μL of 100 mM NH_4HCO_3 buffer (Sigma) was added, followed by centrifugation for 10 min at 14,000 × *g*; we repeated this procedure twice. Next, after adding 40 μL of trypsin buffer (6 μg trypsin in 40 μL NH_4HCO_3 buffer), the samples were shaken at 600 rpm for 1 min and incubated at 37 °C for 16–18 h. The collection tube was replaced and then centrifugated for 10 min at 12,000 × *g*. The filtrate was collected and an amount of 0.1% trifluoroacetic acid (TFA) solution was added, followed by desalination in a C18 Cartridge (Sigma-Aldrich) and OD280 peptide quantification. Finally, approximately 150–180 μg peptides were collected.

2.5. TMT peptide labeling and fractionation

Peptides were labeled with TMT reagents according to the manufacturer's instructions (Thermo Fisher Scientific). To quantify nine samples, each aliquot (100 μg of peptide equivalent) was reacted with one tube of TMT reagent. After the sample was dissolved in 100 μL of 0.05 M tetraethylammonium bromide (TEAB) solution, pH 8.5, the TMT reagent was dissolved in 41 μL of anhydrous acetonitrile. The mixture was incubated at room temperature for 1 h. Then, 8 μL of 5% hydroxylamine was added to the sample and incubated for 15 min to quench the reaction. The 9-plex labeled samples were pooled together and lyophilized.

The TMT-labeled peptides mixture was fractionated using a Waters XBridge BEH130 column (C18, 3.5 μm, 2.1 × 150 mm) on an Agilent 1290 high-performance liquid chromatographer (HPLC) operating at 0.3 mL/min. Buffer A consisted of 10 mM ammonium formate and buffer B consisted of 10 mM ammonium formate with 90% acetonitrile; both buffers were adjusted to pH 10 with ammonium hydroxide. A total of 30 fractions were collected for each peptide mixture and then concatenated to 15 (pooling equal interval RPLC fractions). The fractions were dried for nano LC-MS/MS analysis.

2.6. LC-MS analysis

Separation was performed using an EASY-nLC1200 nanoflow HPLC system (Thermo Fisher Scientific, Karlsruhe, BW, Germany). The buffer used in the analysis included solvent A (0.1% formic acid (FA) in water)

and solvent B (98% acetonitrile) (Merck, 1499230-935) with 0.1% FA. First, 95% solution A was used for equilibration of the column. The sample was loaded onto a Trap column (2 cm × 100 μm, 5 μm-C18) and transferred to a Thermo Scientific EASY analytical column (75 μm × 120 mm, 3 μm-C18) at a 300 nL/min flow rate for separation. The relevant liquid phase gradient was as follows: 0–2 min, linear gradient from 4% to 7% buffer B; 2–67 min, linear gradient from 7% to 20% buffer B; 67–79 min, linear gradient from 20% to 35% buffer B; 79–81 min, linear gradient from 30% to 90% buffer B; and 81–90 min, buffer B maintained at 90%. For LC/MS analysis, the peptides were subjected to tandem MS using a Q-Exactive Plus MS (Thermo Scientific). The parameters were as follows: detection method, positive mode; capillary voltage, 1.8 kV; isolation width, 1.6 Th; and parent ion scanning range recorded in the range of 300–1800 *m/z*. The mass-to-charge ratio of the fragments of the peptides and polypeptides was collected as follows: 20 fragment maps (MS2 scan, high energy collision dissociation (HCD)) were acquired after each full scan, which employed primary MS resolution of 70,000 (at *m/z* 200), AGC target values of 1e6, Level 1 maximum IT of 50 ms, and secondary MS resolution of 35,000 (at *m/z* 200), a target AGC value of 1e5, and Level 2 maximum IT of 50 ms (MS2 Activation Type: HCD; Isolation window: 1.6 Th; Normalized collision energy: 35).

2.7. Database search and protein quantification

The resulting LC-MS/MS raw files were imported into the MaxQuant software program (version 1.6.0.16) for data interpretation and protein identification against the database Uniprot_Hordeum-vulgare_201747-20180125 (released in January 2015 and including 201,747 sequences), which was sourced from the protein database at https://www.uniprot.org/uniprot/?query=Hordeum-vulgare&sort=score. An initial search was set at a precursor mass window of 6 ppm. The search followed an enzymatic cleavage rule of trypsin/P and allowed maximal two missed cleavage sites and a mass tolerance of 20 ppm for fragment ions. The modification set was as follows: fixed modification: carbamidomethyl (C), TMT10plex (K), TMT10plex (*N*-term); and variable modification: oxidation (M) and acetyl (protein *N*-term). The minimum 7 amino acids for peptide, > 1 unique peptide was required per protein. For peptide and protein identification, false discovery rate (FDR) was set to 1%. The TMT reporter ion intensity was used for quantification. The relative quantitative protein analysis of samples was conducted using MaxQuant algorithms (http://www.maxquant.org) (Tyanova, Temu, & Cox, 2016).

2.8. Bioinformatics analysis

Analyses of bioinformatics data were performed with the Perseus software program (Tyanova, Temu, & Sinitcyn, 2016), Microsoft Excel, and R statistical computing software. Differentially expressed proteins (DEPs) were screened in H vs. L, H vs. M, and L vs. M groups, with the cut-off of ratio fold change of > 1.20 or < 0.83 in expression and P-values < 0.05. In addition, DEPs in the H vs. L vs. M groups were identified using one-way analysis of variance (ANOVA). Hierarchical clustering (Euclidean distance) was performed on proteins with significant variance features (FDR q < 0.01), as determined by ANOVA. Expression data were grouped together by hierarchical clustering based on the protein level.

For functional enrichment analysis of the identified proteins, information was extracted from UniProtKB/Swiss-Prot (Boutet et al., 2016), Kyoto Encyclopedia of Genes and Genomes (KEGG) (Kanehisa, Goto, Sato, Furumichi, & Tanabe, 2012), and Gene Ontology (GO) (Ashburner et al., 2000). GO and KEGG enrichment analyses were performed using the Fisher's exact test, and FDR correction for multiple testing was also performed. GO terms were grouped into the following three categories: biological process (BP), molecular function (MF), and cellular component (CC) (Ashburner et al., 2000). The construction of PPI networks was also conducted using the STRING database with the Cytoscape software program (Kohl, Wiese, & Warscheid, 2011).

2.9. Targeted quantification using liquid chromatography-parallel reaction monitoring/mass spectrometry (LC-PRM/MS) and data analysis

Based on the results of the original TMT-based quantitative proteomics analysis, we selected the appropriate target peptides of the candidate proteins and performed targeted shotgun MS to finally determine the peptides of the target proteins with reliable identification information, which could be used for PRM quantification analysis. The peptide information suitable for PRM analysis was imported into the Xcalibur software program for PRM setup. Briefly, a 2-μg peptide from each sample was taken for LC-PRM/MS analysis. After sample loading, chromatographic separation was performed using a Thermo Scientific EASY-nLC nano-HPLC system. The following buffer was used: A solution was 0.1% formic acid aqueous solution and solution B was a mixed solution of 0.1% formic acid, acetonitrile, and water (95% of acetonitrile). The column was first equilibrated with 95% A solution. The sample was injected into a Trap column (100 μm × 20 mm, 5 μm-C18, Dr. Maisch GmbH) and subjected to gradient separation through a chromatography column (75 μm × 150 mm, 3 μm-C18, Dr. Maisch GmbH) at a flow rate of 300 nL/min. The liquid phase separation gradient was as follows: 0 min–2 min, linear gradient of B liquid from 3% to 5%; 2 min–52 min, linear gradient of B liquid from 5% to 25%; 52 min–60 min, linear gradient of B liquid from 25% to 45%; 60 min–65 min, linear gradient of B liquid from 45% to 90%; and 65 min–75 min, B liquid maintained at 90%. The peptides were separated and subjected to targeted PRM/MS using a Q-Exactive Plus mass spectrometer (Thermo Scientific). The analysis time was 75 min. The parameters were set as follows: detection mode: positive mode; parent ion scanning range: 350–1500 *m/z*; capillary voltage, 1.8 kV; isolation width, 1.6 Th; first-order MS resolution: 70,000 @*m/z* 200; AGC target: 3e6; first-level maximum IT: 200 ms. Peptide secondary MS was performed as follows: for each full scan, target peptides of precursor *m/z* were sequentially selected based on the inclusion list for second-order MS (MS2) scan with the parameters as follows: resolution: 35,000 @ *m/z* 200; AGC target: 3e6; Level 2 Maximum IT: 120 ms; MS2 Activation Type: HCD; Peptide fragmentation: nitrogen; Isolation window: 2.0 Th; Normalized collision energy: 27 eV. The obtained PRM data of the raw RAW file was analyzed using the Skyline 4.1 software program.

3. Results

3.1. Total anthocyanin content

The total anthocyanin content varied significantly between purple, blue, and white barley grains (H, M, and L groups, respectively). H group was found to possess the highest anthocyanin content among all three colored grains. The total anthocyanin content distribution was 46.62 ± 3.51 mg/100 g in purple barley (H group) and 8.24 ± 1.78 mg/100 g in blue barley (M group). Anthocyanin could not be detected in white barley (L group) (Fig. 1).

3.2. General information for TMT-LC-MS/MS analysis

The following information regarding proteome data was exported: number of peptide-spectral matches (i.e., several spectra hits for the same peptide), total peptide number, unique peptide number, protein groups, and quantified protein, which were 56,468, 16,909, 14,602, 3564, and 3461, respectively. A boxplot of normalized density is shown in Fig. 2A. In addition, pairwise Pearson's correlation coefficients of all nine samples (three replicates × three groups) were obtained to evaluate the repeatability of protein relative quantitation, with the results showing high reproducibility (R > 0.99) (Fig. 2B).

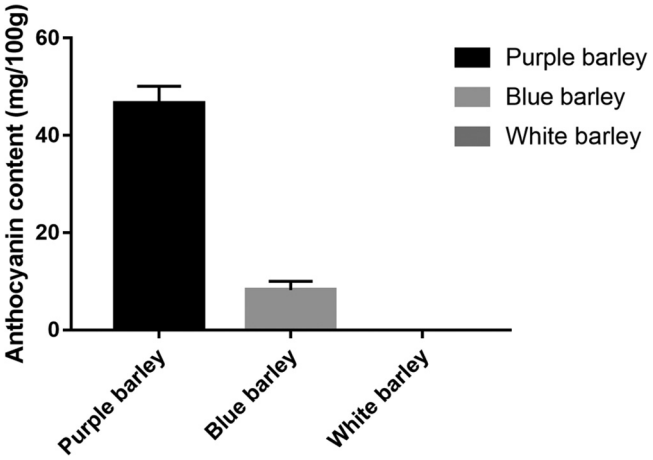

Fig. 1. Total anthocyanin content in purple, blue, and white barley. The anthocyanin content in purple was significantly higher than that in blue. And anthocyanins could not be detected in white barley.

3.3. Comparative analysis of protein expression in different groups

The screen comparing H and L groups identified 297 DEPs, of which 155 were upregulated and 142 were downregulated. The comparison between the H and M groups identified 300 DEPs, of which 162 were upregulated and 138 were downregulated. In addition, 254 DEPs were found in the L vs. M group, including 155 upregulated and 99 downregulated proteins. Moreover, we identified 1421 DEPs in the H vs. L vs. M group using ANOVA. All proteins are shown in Supplementary Table 1. The volcano plots and heatmaps of DEPs in H vs. L, H vs. M, and L vs. M groups are shown in Fig. 2 and Supplementary Fig. 1.

3.4. Functional enrichment analysis of DEPs

We then predicted the functions of DEPs in different comparison groups by bioinformatics analyses. The results showed that the proteins could be assigned to different GO terms for BP, CC, and MF categories (Fig. 3). The prominent GO terms for BP enriched by DEPs in H vs. L, H vs. M, L vs. M, and H vs. M vs. L groups were the small molecule metabolic process, organonitrogen compound biosynthetic and metabolic process, and single-organism metabolic process. The top GO CC categories that were enriched by these proteins included the cytoplasm, and the intracellular and cell components. Bioinformatics analyses also

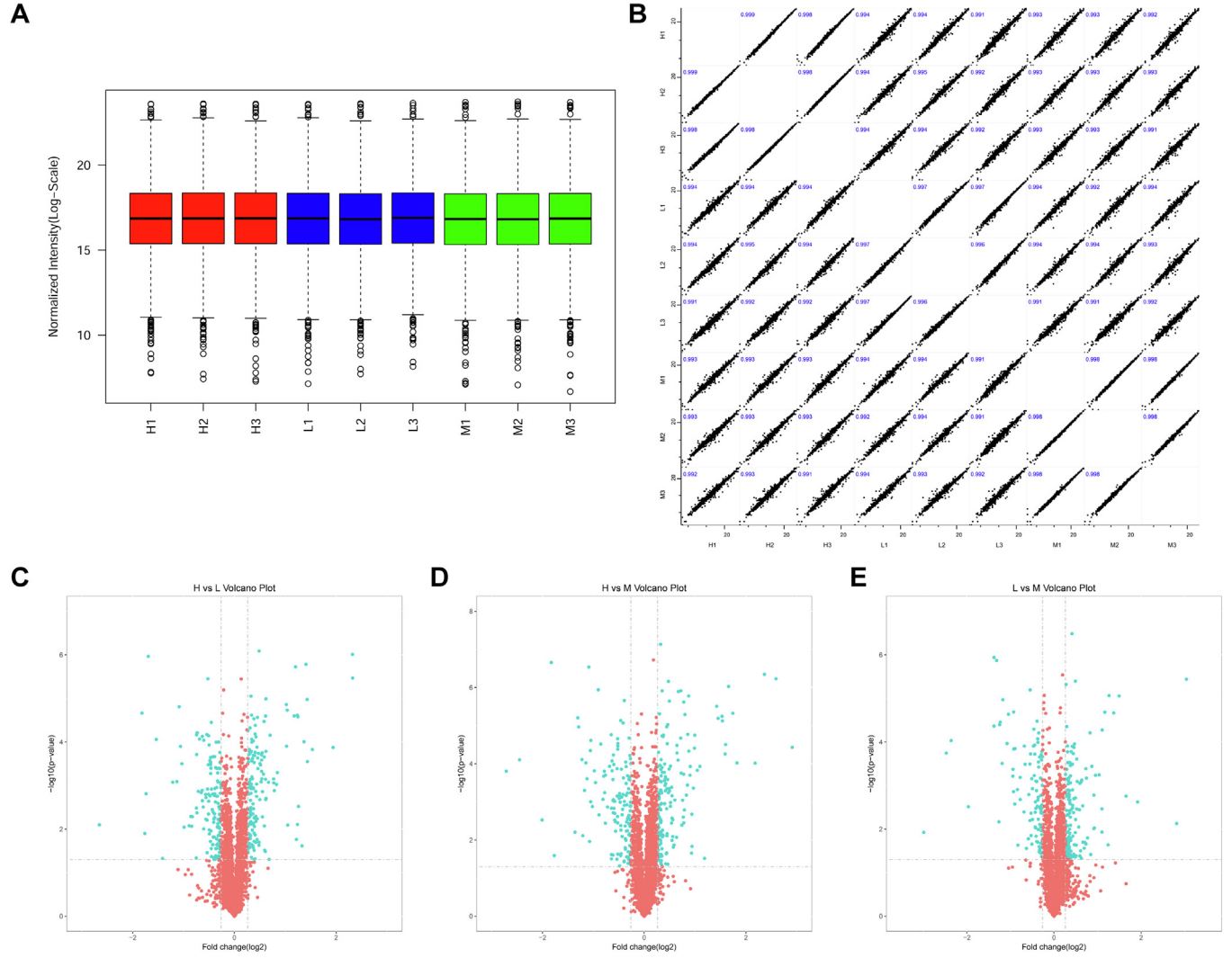

Fig. 2. Volcano plots and heatmaps of proteins with differential expression in H vs. L, H vs. M, and L vs. M groups. A, Boxplot of normalized density. B, Pearson's correlation of normalized densities. C, volcano plots of proteins with differential expression in H vs. L, H vs. M, and L vs. M groups. Green dots indicate proteins with differential expression. (For interpretation of the references to color in this figure legend, the reader is referred to the web version of this article.)

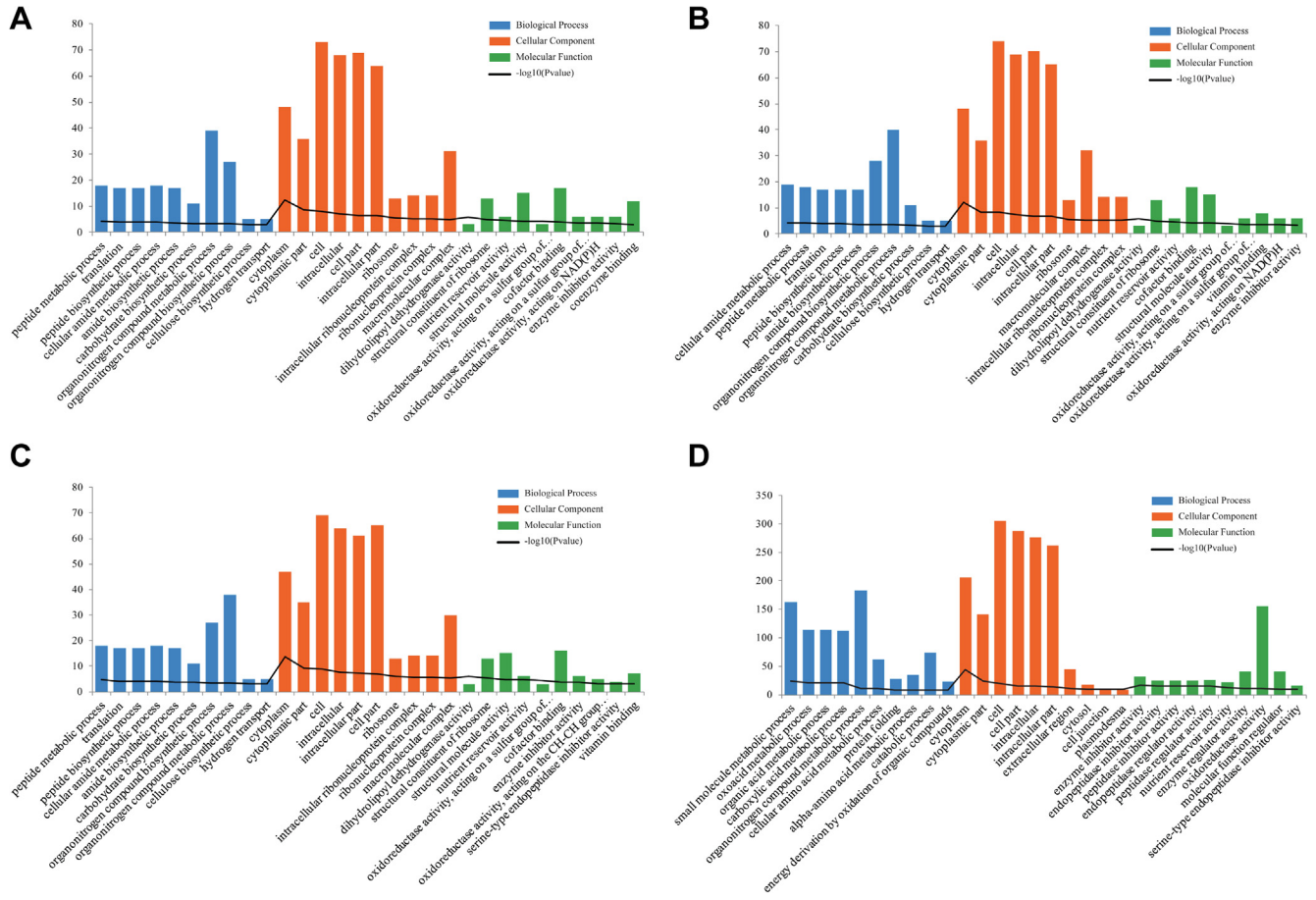

Fig. 3. Gene ontology (GO) term enrichment for differentially expressed proteins. A, B, C, and D, GO terms (including biological process, cellular component, and molecular function) enriched by proteins with differential expression in H vs. L (A), H vs. M (B), L vs. M (C), and H vs. M vs. L (D) groups, respectively.

indicated that these DEPs were associated with oxidoreductase activity, structural constituents of ribosomes, structural molecule activity, and cofactor binding. In addition, the proteins with differential expression underwent KEGG analysis, and the results showed that H vs. L, H vs. M, L vs. M, and H vs. M vs. L groups were mainly involved in carbon metabolism, oxidative phosphorylation, ribosome, protein processing in endoplasmic reticulum, metabolic pathways, and the biosynthesis of amino acids and secondary metabolites (Supplementary Fig. 2).

3.5. PPI network construction of DEPs

To further investigate the functions of these proteins, PPI networks were constructed on proteins with differential expression in H vs. L, H vs. M, L vs. M, and H vs. M vs. L groups. As shown in Fig. 4A, in the PPI network of the DEPs in the H vs. L group, proteins such as MUBI (downregulated; ubiquitin-40S ribosomal protein), A0A287IFH6 (upregulated; uncharacterized protein), and F2CY09 (upregulated; predicted protein) had a high degree of connectivity, which indicated more interactions with other proteins. In the PPI network of DEPs in the H vs. M group (Fig. 4B), F2D355 (upregulated; predicted protein), A0A1C9ZNX9 (upregulated; ATP synthase subunit alpha), and F2CY09 (upregulated; predicted protein) had a relatively high degree of connectivity. In addition, F2D355 (upregulated; predicted protein), A0A287IFH6 (upregulated; uncharacterized protein), and A0A287EYB0 (downregulated; uncharacterized protein) had a high degree of connectivity in the PPI network of DEPs in the L vs. M group (Fig. 4C). Moreover, PPI analysis was performed on the proteins with differential protein that were identified in the H vs. M vs. L group (Fig. 4D). Combined with these four PPI networks, the proteins A0A287F6S1 (uncharacterized protein), A0A287E139 (succinate dehydrogenase (ubiquinone) flavoprotein subunit, mitochondrial), M0VD47 (uncharacterized protein), A0A287F1X0 (uncharacterized protein), M0XDX5 (uncharacterized protein), and F5B7F0 (acetolactate synthase (fragment)) were found in all four networks and had a relatively high degree of connectivity.

3.6. Cluster analysis of protein expression patterns in the H vs. M vs. L groups

The proteins identified in the H vs. M vs. L groups (Fig. 5A) were divided into six clusters based on their expression patterns (Fig. 5B, Supplementary Table 2). The protein expression patterns in cluster 1 from the H vs. L group were downregulated. Downregulation in the M vs. H group was identified with respect to proteins of cluster 2; however, there was upregulation in the L vs. M group. A slight upregulation in the M vs. H group was found for the proteins of cluster 3, and downregulation in the L vs. M group, whereas the proteins in cluster 4 were upregulated in the M vs. H group but downregulated slightly in the L vs. M group. Moreover, protein expression patterns of cluster 5 in the H vs. M group were slightly downregulated; however, they were upregulated in the L vs. M group. Lastly, the protein expression patterns in cluster 6 from the H vs. L group were upregulated.

To gain further understanding of the mechanisms and biological functions of proteins from the six clusters, GO and pathway analyses were performed (Supplementary Fig. 3). In the six clusters, 'single-organism metabolic process,' 'small molecule metabolic process,' 'defense response,' 'carbohydrate derivative metabolic process,' and 'cellular catabolic process' were the most important terms for the BP category;

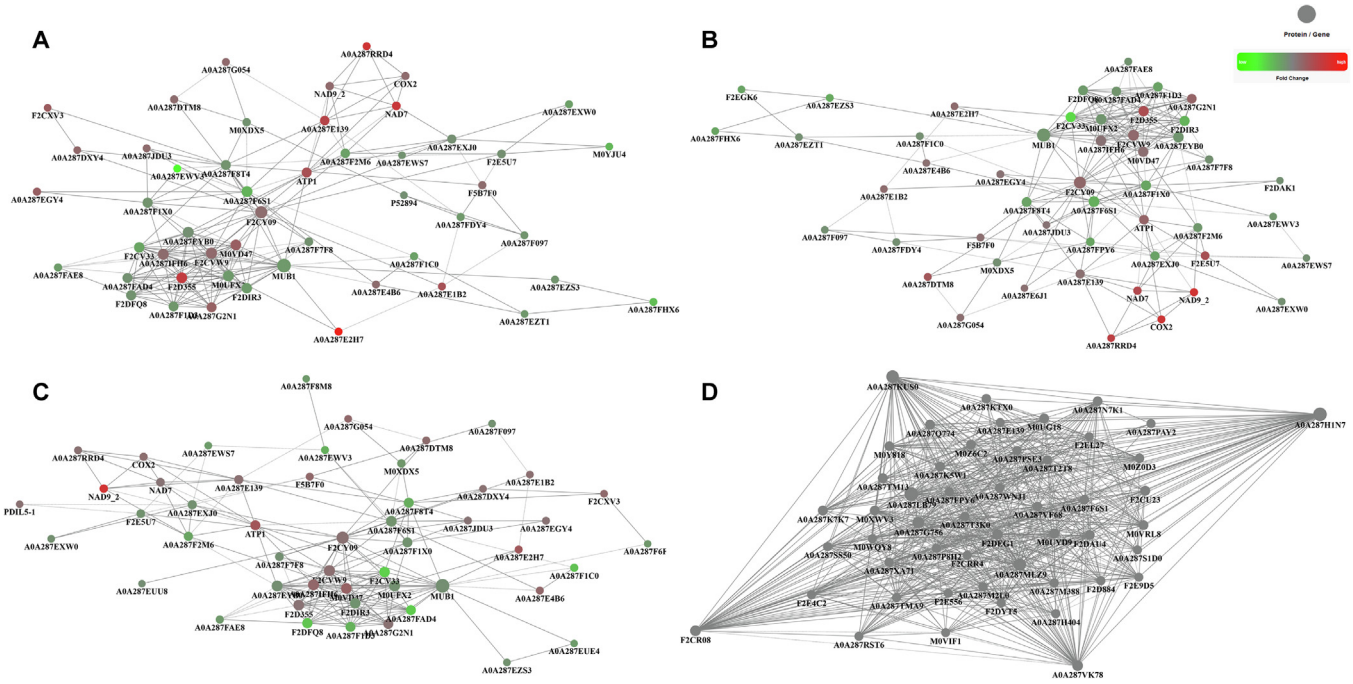

Fig. 4. Protein-protein interaction (PPI) networks of differentially expressed proteins (DEPs). PPI networks enriched by DEPs in H vs. L, H vs. M, L vs. M, and H vs. M vs. L groups. Red nodes indicate upregulated proteins and green nodes indicate downregulated proteins. The shade of color indicates different changes in fold expression of proteins. (For interpretation of the references to color in this figure legend, the reader is referred to the web version of this article.)

'cytoplasmic part,' 'cell part,' and 'intracellular part' were the most important terms for the CC category; and 'cofactor binding,' 'catalytic activity,' and 'enzyme regulator activity' were the most important terms for the MF category. KEGG enrichment analysis showed the main pathways as carbon metabolism, biosynthesis of amino acids, metabolic pathways, and biosynthesis of secondary metabolites.

Further, a PPI network was constructed of the proteins from these six clusters and the associated functions displayed on the PPI networks (Fig. 6), which presented the significant functions affected by different protein expression patterns. The proteins in cluster 1 were mainly associated with amino acid biosynthesis, carbon metabolism, pyruvate metabolism, metabolic pathways, and biosynthesis of secondary metabolites, including F2ELT5 (malic enzyme), F2CV88 (40S ribosomal protein S26), A0A287GW56 (pyruvate dehydrogenase E1 component subunit alpha), F5B7F0 (acetolactate synthase (fragment)), P52894 (alanine aminotransferase 2), and A0A287WNJ1 (malate dehydrogenase). Proteins in cluster 2 were mainly associated with the biosynthesis of amino acids and secondary metabolites, and glyoxylate and dicarboxylate metabolism, such as A0A287N3J4 (glutamine synthetase), A0A287SQZ2 (methylenetetrahydrofolate reductase), F2DKD7 (pyruvate dehydrogenase E1 component subunit alpha), Q94IC0 (betaine aldehyde dehydrogenase), M0UG18 (citrate synthase), A0A287G756 (delta-1-pyrroline-5-carboxylate synthase), and A0A287Q774 (malate dehydrogenase). Proteins in cluster 3 were associated with the pentose phosphate pathway, endocytosis, metabolic pathways, carbon fixation in photosynthetic organisms, carbon metabolism, and the biosynthesis of amino acids and secondary metabolites including A0A287TTB0 (phosphoglycerate kinase) and M0Z0D3 (malate dehydrogenase). Proteins in cluster 4 were involved in amino sugar and nucleotide sugar metabolism, glycolysis/gluconeogenesis, carbon fixation in photosynthetic organisms, protein processing in the endoplasmic reticulum, protein export, and pyruvate metabolism, such as A0A287US34 (pyruvate dehydrogenase E1 component subunit alpha), Q1PBI4 (glucose-6-phosphate isomerase), and F2DCT3 (pyrophosphate–fructose 6-phosphate 1-phosphotransferase subunit alpha). Proteins in cluster 5 were involved in amino sugar and nucleotide sugar metabolism, metabolic pathways, carbon metabolism, oxidative phosphorylation, and proteasome, including Q9ZRI8 (formate dehydrogenase, mitochondrial), M0VN24 (isocitrate lyase), A0A287F2M6 (ATP synthase subunit gamma), A0A287S239 (proteasome subunit alpha type), and A0A287KTX0 (pyruvate kinase). Finally, proteins in cluster 6 were associated with the biosynthesis of secondary metabolites, protein processing in the endoplasmic reticulum, metabolic pathways, carbon metabolism, and phenylpropanoid biosynthesis, including F2DBE3 (catalase), F2DAK8 (predicted protein), F2CPZ4 (acyl-coenzyme A oxidase), F2CU23 (glyceraldehyde-3-phosphate dehydrogenase), and F2CXV3 (nucleoside diphosphate kinase).

3.7. Validation of the expression pattern of the TMT using PRM

To assess the validity of the TMT data, we randomly selected six proteins for validation using PRM. As shown in Fig. 7, the PRM results showed good correlation with the TMT data. A0A287E139 (succinate dehydrogenase (ubiquinone) flavoprotein subunit, mitochondrial), A0A287G756 (delta-1-pyrroline-5-carboxylate synthase), and M0UG18 (citrate synthase) had the lowest expression in the groups. In addition, the levels of F2CXV3 (nucleoside diphosphate kinase) and F2CU23 (glyceraldehyde-3-phosphate dehydrogenase) that belonged to cluster 6 increased in the H vs. L group. The expression levels of M0Z0D3 (malate dehydrogenase) were higher in the M group than those in the H group and L group.

4. Discussion

The accumulation of different pigments in the pericarp, lemma, and aleurone layer contributes to the color of barley grains (Strygina et al., 2017). However, limited information is available regarding the mechanisms underlying anthocyanin biosynthesis in barley with different colors. In the present study, TMT-LC-MS/MS-based quantitative proteome analysis showed protein changes in the metabolic processes of grains in purple, blue, and white barley. These proteins were mainly associated with carbon metabolism, carbon fixation in photosynthetic organisms, biosynthesis of amino acids, metabolic pathways, protein processing and transport, and synthesis of secondary metabolites.

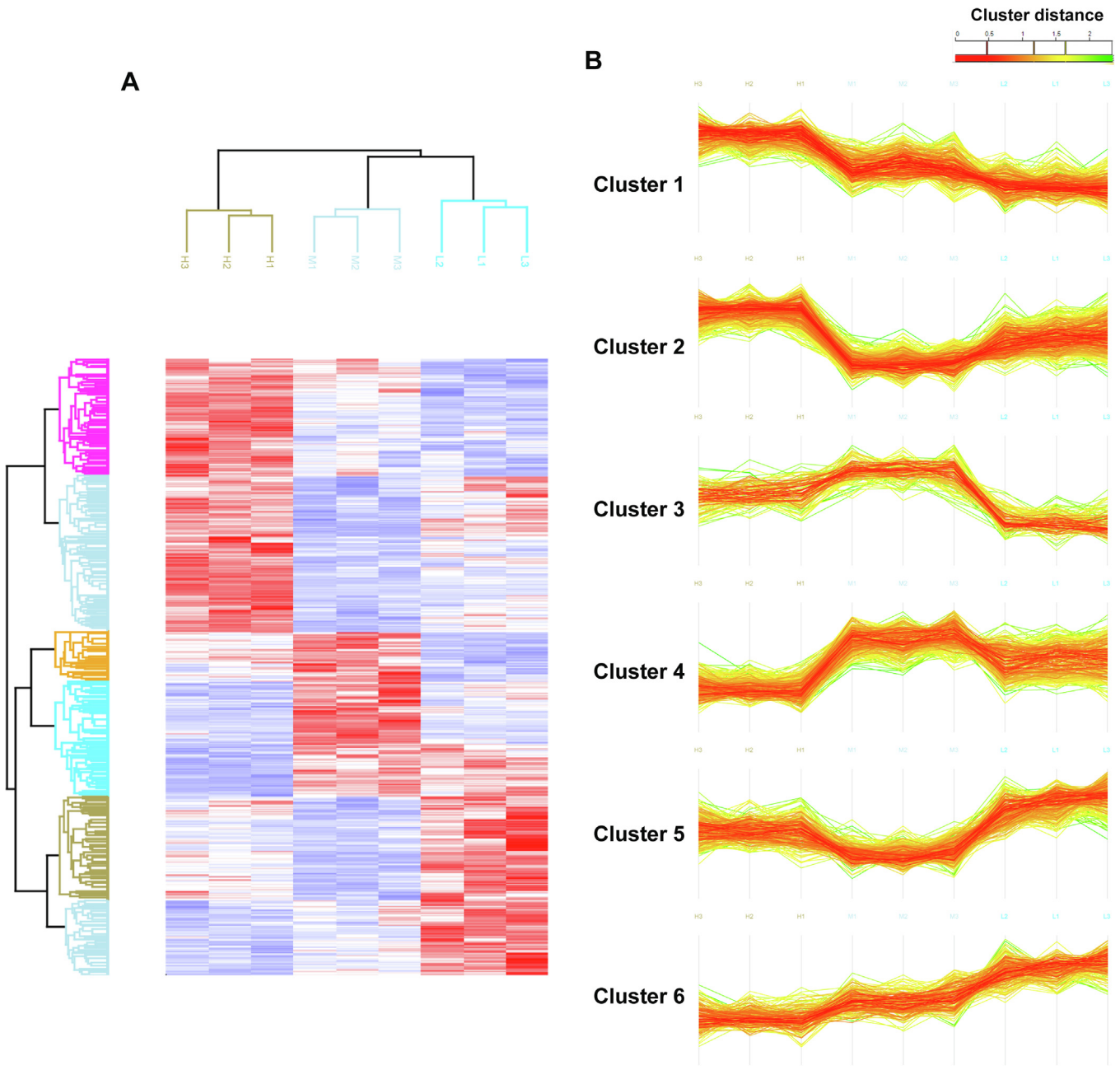

Fig. 5. Heatmaps and clustering analysis of DEPs in H vs. M vs. L group. A, Heatmaps of DEPs in H vs. M vs. L groups. B, Six clusters identified by the DEPs based on expression levels.

Taken together, our research will provide a basis for the further study on the improvement of anthocyanin content in barley.

Anthocyanins are biosynthesized via the phenylpropanoid metabolism pathway, of which the first committed step is the conversion of phenylalanine into *trans*-cinnamic acid in the presence of phenylalanine ammonia lyase, which then diverges into various branches at ρ-coumaroyl CoA (Shen et al., 2016). Malonyl-CoA and coumaroyl CoA are precursors for the synthesis of all flavonoids, including anthocyanins (Ewaschuk et al., 2012). Chalcone synthase catalyzes the first committed step in the flavonoid skeleton by condensing p-coumaryl-CoA with three molecules of acetyl-CoA derived from malonyl-CoA to form chalcone. This is followed by the stereospecific and intramolecular cyclization of chalcone into flavanone by chalcone-flavanone isomerase (Park et al., 2018). In the present study, we found the M0ZAZ3 (chalcone-flavanone isomerase family protein) was differentially expressed in H vs L, H vs M, and L vs M groups (Supplementary Table 1), which indicated different activity of chalcone-flavanone isomerase in the three barley varieties. Furthermore, pathway enrichment analysis showed the proteins, including F5B7F0 (acetolactate synthase (fragment)), A0A287N3J4 (glutamine synthetase), and F2CPZ4 (acyl-coenzyme A oxidase) in significant clusters were also involved in the phenylpropanoid biosynthesis pathway and the biosynthesis of amino acids, which was consistent with the results of previous studies suggesting that proteins involved in amino acid metabolism are associated with anthocyanin biosynthesis (Sima et al., 2018). Among these proteins, glutamine synthetase 1 and glutamine synthetase 2 have been reported to play important role in developing rice grain and carbon-nitrogen metabolic balance (Chen et al., 2014; Thandapilly et al., 2018). Moreover, carbon-nitrogen metabolic balance has been shown to play a major role in regulating anthocyanin content in *Arabidopsis* (Naceur et al., 2017). Hence, we speculated that A0A287N3J4 (glutamine synthetase) might play a critical role in the anthocyanin biosynthesis in barley through

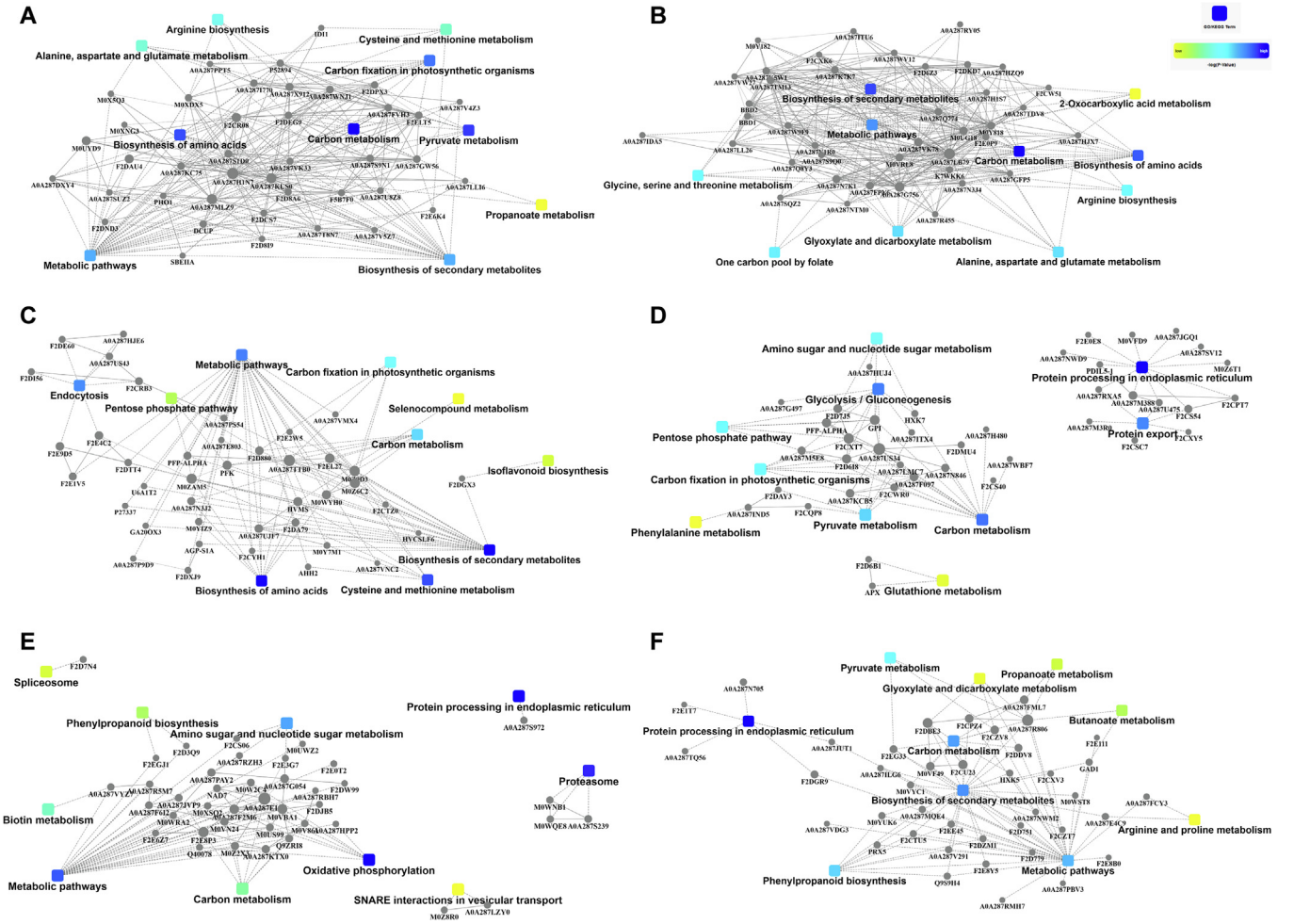

Fig. 6. PPI networks of proteins in six clusters. A, B, C, D, E, and F represent proteins in cluster 1, 2, 3, 4, 5, and 6, respectively. The rectangular node represents the KEGG pathway/biological process. The P-value is represented by a yellow-blue gradient color; the yellow color indicates a small P-value and the blue color indicates a large P-value. (For interpretation of the references to color in this figure legend, the reader is referred to the web version of this article.)

regulating the carbon-nitrogen metabolic balance; however, its molecular mechanism in anthocyanin biosynthesis still needs to be investigated in future studies.

Carbohydrates or sugars provide building blocks for plant structural components in addition to being the primary source of energy during plant growth (Villar-Salvador, Uscola, & Jacobs, 2015). Previous studies have reported that carbohydrates have stimulatory effects on the synthesis of anthocyanin in many plant species (Wan, Zhang, Song, Tian, & Yao, 2015) and have shown the enhancement of anthocyanin biosynthesis by sugar (Hara, Oki, Hoshino, & Kuboi, 2003; Solfanelli, Poggi, Loreti, Alpi, & Perata, 2006). In the present study, pyruvate metabolism, glyoxylate and dicarboxylate metabolism, and glycolysis/gluconeogenesis, which were associated with sugar metabolism, were also significantly enriched by the DEPs. Pyruvate, the product from glycolysis, can be transformed into acetyl-CoA by a process called pyruvate decarboxylation (Sweetlove, Beard, Nunes-Nesi, Fernie, & Ratcliffe, 2010). In addition, acetyl-CoA is a substrate for the TCA cycle that leads to the synthesis of flavanols and anthocyanin (Lin et al., 2017). A previous study demonstrated that the TCA cycle intermediate 2-oxoglutarate (2-OG) and 2-OG dependent dioxygenases plays important roles in glucosinolate, flavonoid, and alkaloid metabolism (Araujo, Martins, Fernie, & Tohge, 2014). In the present study, proteins such as F2ELT5 (malic enzyme), A0A287WNJ1 (malate dehydrogenase), A0A287GW56 (pyruvate dehydrogenase E1 component subunit alpha), A0A287WNJ1 (malate dehydrogenas), M0UG18 (citrate synthase), A0A287Q774 (malate dehydrogenase), M0Z0D3 (malate dehydrogenase), A0A287US34 (pyruvate dehydrogenase E1 component subunit alpha), A0A287KTX0 (pyruvate kinase), and F2CPZ4 (acyl-coenzyme A oxidase), which are associated with the TCA cycle showed different expression changes in barley with different colors. Thus, these proteins might affect the biosynthesis and accumulation of anthocyanin in barley via TCA cycle regulation, which has not been reported till now.

Gluconeogenesis is a metabolic process that leads to the generation of glucose, which can induce anthocyanin accumulation in many plant species (Hu et al., 2016). In the present study, several proteins including A0A287TTB0 (phosphoglycerate kinase), Q1PBI4 (glucose-6-phosphate isomerase), F2DCT3 (pyrophosphate–fructose 6-phosphate 1-phosphotransferase subunit alpha), and F2CU23 (glyceraldehyde-3-phosphate dehydrogenase) were found to be significantly enriched in glycolysis/gluconeogenesis. Actually, in plants, phosphoglycerate kinase participates in the reverse reaction in gluconeogenesis (Rosa-Téllez et al., 2018). And the glucose-6-phosphate isomerase, universally distributed among Eukaryotes, Bacteria, and some Archaea, has an essential function in both catabolic glycolysis and anabolic gluconeogenesis (Grauvogel, Brinkmann, & Petersen, 2007). However, the relationship between the proteins and gluconeogenesis in anthocyanin synthesis still remains unclear. Based on the module analysis from PPI network, our data indicated speculated that proteins associated with gluconeogenesis contributed to different anthocyanin accumulation in purple, blue, and white barley. Similarly, as an important stimulus for anthocyanin biosynthesis and photosynthesis, light is contributes to the

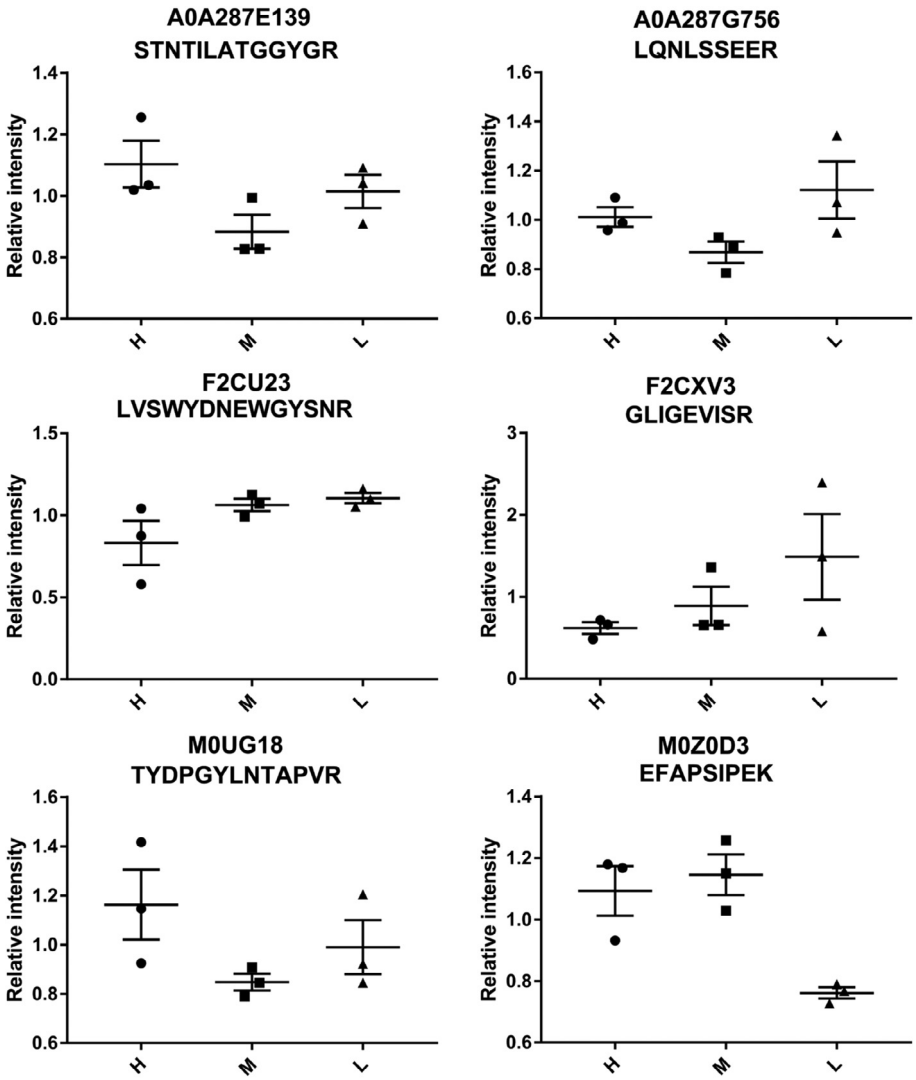

Fig. 7. A regulative model for proteins related to anthocyanin biosynthesis in barley (A) and parallel reaction monitoring (PRM) validation of several proteins identified by the TMT data (A).

formation of anthocyanin (Shen et al., 2016). In our study, several proteins of cluster 4 were involved in the function of carbon fixation in photosynthetic organisms, including A0A287LMC7 (uncharacterized protein), A0A287KCB5 (malic enzyme), F2CXT7 (fructose-bisphosphate aldolase), F2D6I8 (glyceraldehyde-3-phosphate dehydrogenase), A0A287F097 (malic enzyme), and A0A287M5E8 (uncharacterized protein). Thus, we speculated these proteins might be involved in carbon fixation in photosynthetic organisms, and thus contribute to the biosynthesis of anthocyanin in barley.

However, there are still some limitations in our study. First, the L3 replicate showed differences compared to the other two replicates in the heatmap; however, they were still clustered together. More samples should be included in future studies to verify these results. Second, only seed grains upon maturity were harvested and selected for analysis in the present study. Our future research focus will shift to the changes and mechanisms of anthocyanins in these highland barley varieties during different time periods.

5. Conclusion

In conclusion, the differences in protein expression levels in purple, blue, and white barley with different anthocyanin content were investigated using TMT-LC-MS/MS-based quantitative proteome analysis. The results indicated that the proteins associated with carbon metabolism, amino acid biosynthesis, metabolic pathways, and phenylpropanoid biosynthesis significantly promoted anthocyanin biosynthesis in barley, and were the main factors influencing the color differences in these three barley varieties. Our findings provide useful information for better understanding of the global structure of the metabolic network involved in anthocyanin biosynthesis and accumulation in hulless barley, as well as provide a basis for the further study on the improvement of anthocyanin content in barley.

Declarations

Ethics approval and consent to participate

Not applicable.

Consent for publication

Not applicable.

Availability of data and materials

Not applicable. This study constitutes preliminary research and

further study is in progress.

Funding

This work was supported by Financial Special Fund (Program No. 2017CZZX001; XZNKY-2018-C-021), Tibet Department of Major Projects (Program No. XZ201801NA01), Natural Science Foundation of China (Program No. 31760381; 31560441), Anhui Polytechnic University Young and Middle-aged Talents Project (2018–2019) and Natural Science Foundation of Tibet (Program No. XZ2017ZRG-26; XZ2018ZRG-63), Sponsored by AHPU (grant numbers: 2018YQQ011).

Authors' contributions

Conception and design of the research: T. N., W. X. and G. Z.
Acquisition of data: X. Z. and J. D.
Analysis and interpretation of data: Q. X., Y. W., and H. Y.
Statistical analysis: K. Y. and Y. Q.
Drafting the manuscript: G. Z. and T. N.
Revision of manuscript for important intellectual content: G. Z.
All authors have read and approved the manuscript.

Declaration of Competing Interest

The authors declare that they have no known competing financial interests or personal relationships that could have appeared to influence the work reported in this paper.

Acknowledgement

None.

Appendix A. Supplementary data

Supplementary data to this article can be found online at https://doi.org/10.1016/j.foodchem.2019.124973.

References

Abdel-Aal, E.-S. M., Young, J. C., & Rabalski, I. (2006). Anthocyanin composition in black, blue, pink, purple, and red cereal grains. *Journal of Agricultural and Food Chemistry, 54*(13), 4696–4704.

Abdel-Aal, E. S., & Hucl, P. (1999). A rapid method for quantifying total anthocyanins in blue aleurone and purple pericarp wheats. *Cereal Chemistry, 76*(3), 350–354.

Araujo, W. L., Martins, A. O., Fernie, A. R., & Tohge, T. (2014). 2-Oxoglutarate: Linking TCA cycle function with amino acid, glucosinolate, flavonoid, alkaloid, and gibberellin biosynthesis. *Frontiers in Plant Science, 5*(552).

Ashburner, M., Ball, C. A., Blake, J. A., Botstein, D., Butler, H., Cherry, J. M., ... Sherlock, G. (2000). Gene ontology: Tool for the unification of biology. The Gene Ontology Consortium. *Nature Genetics, 25*(1), 25–29.

Avin, A., Levy, M., Porat, Z., & Abramson, J. (2017). Quantitative analysis of protein-protein interactions and post-translational modifications in rare immune populations. *Nature Communications, 8*(1), 1524.

Boutet, E., Lieberherr, D., Tognolli, M., Schneider, M., Bansal, P., Bridge, A. J., ... Xenarios, I. (2016). UniProtKB/Swiss-prot, the manually annotated section of the UniProt knowledge base: How to use the entry view. *Methods in Molecular Biology, 1374*, 23–54.

Chen, X., Long, H., Gao, P., Deng, G., Pan, Z., Liang, J., ... Yu, M. (2014). Transcriptome assembly and analysis of Tibetan hulless barley (Hordeum vulgare L. var. nudum) developing grains, with emphasis on quality properties. *PLoS ONE, 9*(5), e98144.

Ewaschuk, J., Johnson, I., Madsen, K., Vasanthan, T., Ball, R., & Field, C. (2012). Barley-derived β-glucans increases gut permeability, ex vivo epithelial cell binding to E. coli, and naive T-cell proportions in weanling pigs. *Journal of Animal Science, 90*(8), 2652–2662.

Finnie, C., Melchior, S., Roepstorff, P., & Svensson, B. (2002). Proteome analysis of grain filling and seed maturation in barley. *Plant Physiology, 129*(3), 1308–1319.

Glagoleva, A. Y., Shmakov, N. A., Shoeva, O. Y., Vasiliev, G. V., Shatskaya, N. V., Börner, A., ... Khlestkina, E. K. (2017). Metabolic pathways and genes identified by RNA-seq analysis of barley near-isogenic lines differing by allelic state of the Black lemma and pericarp (Blp) gene. *BMC Plant Biology, 17*(1), 182.

Grauvogel, C., Brinkmann, H., & Petersen, J. (2007). Evolution of the glucose-6-phosphate isomerase: The plasticity of primary metabolism in photosynthetic eukaryotes. *Molecular Biology and Evolution, 24*(8), 1611–1621.

Hara, M., Oki, K., Hoshino, K., & Kuboi, T. (2003). Enhancement of anthocyanin biosynthesis by sugar in radish (Raphanus sativus) hypocotyl. *Plant Science, 164*(2), 259–265.

Hu, D.-G., Sun, C.-H., Zhang, Q.-Y., An, J.-P., You, C.-X., & Hao, Y.-J. (2016). Glucose sensor MdHXK1 phosphorylates and stabilizes MdbHLH3 to promote anthocyanin biosynthesis in apple. *PLoS Genetics, 12*(8), e1006273.

Kanehisa, M., Goto, S., Sato, Y., Furumichi, M., & Tanabe, M. (2012). KEGG for integration and interpretation of large-scale molecular data sets. *Nucleic Acids Research, 40*(Database issue), D109–D114.

Kim, M.-J., Hyun, J.-N., Kim, J.-A., Park, J.-C., Kim, M.-Y., Kim, J.-G., ... Chung, I.-M. (2007). Relationship between phenolic compounds, anthocyanins content and antioxidant activity in colored barley germplasm. *Journal of Agricultural and Food Chemistry, 55*(12), 4802–4809.

Kohl, M., Wiese, S., & Warscheid, B. (2011). Cytoscape: Software for visualization and analysis of biological networks. *Methods in Molecular Biology, 696*, 291–303.

Lao, F., Sigurdson, G. T., & Giusti, M. M. (2017). Health benefits of purple corn (Zea mays L.) phenolic compounds. *Comprehensive Reviews in Food Science and Food Safety, 16*(2), 234–246.

Lin, M., Fang, J., Qi, X., Li, Y., Chen, J., Sun, L., & Zhong, Y. (2017). iTRAQ-based quantitative proteomic analysis reveals alterations in the metabolism of Actinidia arguta. *Scientific Reports, 7*(1), 5670.

Mullick, D., Faris, D., Brink, V., & Acheson, R. (1958). Anthocyanins and anthocyanidins of the barley pericarp and aleurone tissues. *Canadian Journal of Plant Science, 38*(4), 445–456.

Naceur, A. B., Cheikh-M'hamed, H., da Silva, J. A. T., & Abdelly, C. (2017). The response of two naked barley varieties (Hordeum vulgare L.) to four phosphorus fertilizer levels. *Journal of Agricultural and Crop Research, 5*(2), 17–24.

Naryzhny, S. (2018). Inventory of proteoforms as a current challenge of proteomics: Some technical aspects. *Journal of Proteomics*.

Pan, S., & Aebersold, R. (2007). Quantitative proteomics by stable isotope labeling and mass spectrometry. *Mass spectrometry data analysis in proteomics* (pp. 209–218). Springer.

Park, S., Lee, C., Cho, S., Lee, H., Park, H., Lee, J., & Lee, J. (2018). Crystal structure and enzymatic properties of chalcone isomerase from the Antarctic vascular plant Deschampsia antarctica Desv. *PLoS ONE, 13*(2), e0192415.

Rauniyar, N. (2015). Parallel reaction monitoring: A targeted experiment performed using high resolution and high mass accuracy mass spectrometry. *International Journal of Molecular Sciences, 16*(12), 28566–28581.

Ronsein, G. E., Pamir, N., von Haller, P. D., Kim, D. S., Oda, M. N., Jarvik, G. P., ... Heinecke, J. W. (2015). Parallel reaction monitoring (PRM) and selected reaction monitoring (SRM) exhibit comparable linearity, dynamic range and precision for targeted quantitative HDL proteomics. *Journal of Proteomics, 113*, 388–399.

Rosa-Téllez, S., Anoman, A., Flores-Tornero, M., Toujani, W., Alseek, S., Fernie, A., ... Ros, R. (2018). Phosphoglycerate kinases are co-regulated to adjust metabolism and to optimize growth. *Plant Physiology, 176*(2), 1182–1198.

Shen, Q., Fu, L., Dai, F., Jiang, L., Zhang, G., & Wu, D. (2016). Multi-omics analysis reveals molecular mechanisms of shoot adaption to salt stress in Tibetan wild barley. *BMC Genomics, 17*(1), 889.

Shoeva, O. Y., Mock, H. P., Kukoeva, T. V., Borner, A., & Khlestkina, E. K. (2016). Regulation of the flavonoid biosynthesis pathway genes in purple and black grains of hordeum vulgare. *PLoS ONE, 11*(10), e0163782.

Sima, P., Vannucci, L., & Vetvicka, V. (2018). β-glucans and cholesterol. *International Journal of Molecular Medicine, 41*(4), 1799–1808.

Solfanelli, C., Poggi, A., Loreti, E., Alpi, A., & Perata, P. (2006). Sucrose-specific induction of the anthocyanin biosynthetic pathway in Arabidopsis. *Plant Physiology, 140*(2), 637–646.

Strygina, K. V., Borner, A., & Khlestkina, E. K. (2017). Identification and characterization of regulatory network components for anthocyanin synthesis in barley aleurone. *BMC Plant Biology, 17*(Suppl 1), 184.

Stuper-Szablewska, K., & Perkowski, J. (2017). Phenolic acids in cereal grain: Occurrence, biosynthesis, metabolism and role in living organisms. *Critical Reviews in Food Science and Nutrition,* 1–12.

Sweetlove, L. J., Beard, K. F., Nunes-Nesi, A., Fernie, A. R., & Ratcliffe, R. G. (2010). Not just a circle: Flux modes in the plant TCA cycle. *Trends in Plant Science, 15*(8), 462–470.

Thandapilly, S. J., Ndou, S. P., Wang, Y., Nyachoti, C. M., & Ames, N. P. (2018). Barley beta-glucan increases fecal bile acid excretion and short chain fatty acid levels in mildly hypercholesterolemic individuals. *Food & Function, 9*(6), 3092–3096.

Thompson, A., Schäfer, J., Kuhn, K., Kienle, S., Schwarz, J., Schmidt, G., ... Hamon, C. (2003). Tandem mass tags: A novel quantification strategy for comparative analysis of complex protein mixtures by MS/MS. *Analytical Chemistry, 75*(8), 1895–1904.

Tyanova, S., Temu, T., & Cox, J. (2016). The MaxQuant computational platform for mass spectrometry-based shotgun proteomics. *Nature Protocols, 11*(12), 2301–2319.

Tyanova, S., Temu, T., & Sinitcyn, P. (2016). The Perseus computational platform for comprehensive analysis of (prote)omics data. *Nature Methods, 13*(9), 731–740.

Villar-Salvador, P., Uscola, M., & Jacobs, D. F. (2015). The role of stored carbohydrates and nitrogen in the growth and stress tolerance of planted forest trees. *New Forests, 46*(5–6), 813–839.

Wan, H., Zhang, J., Song, T., Tian, J., & Yao, Y. (2015). Promotion of flavonoid biosynthesis in leaves and calli of ornamental crabapple (Malus sp.) by high carbon to nitrogen ratios. *Frontiers in Plant Science, 6*, 673.

Wiśniewski, J. R. (2016). Quantitative evaluation of filter aided sample preparation (FASP) and multienzyme digestion FASP protocols. *Analytical Chemistry, 88*(10), 5438–5443.

Zhu, F. (2018). Anthocyanins in cereals: Composition and health effects. *Food Research International, 109*, 232–249.